AEM
Journals.ASM.org

Effects of Iron and Nitrogen Limitation on Sulfur Isotope Fractionation during Microbial Sulfate Reduction

Min Sub Sim,* Shuhei Ono, and Tanja Bosak

Department of Earth, Atmospheric, and Planetary Sciences, Massachusetts Institute of Technology, Cambridge, Massachusetts, USA

Sulfate-reducing microbes utilize sulfate as an electron acceptor and produce sulfide that is depleted in heavy isotopes of sulfur relative to sulfate. Thus, the distribution of sulfur isotopes in sediments can trace microbial sulfate reduction (MSR), and it also has the potential to reflect the physiology of sulfate-reducing microbes. This study investigates the relationship between the availability of iron and reduced nitrogen and the magnitude of S-isotope fractionation during MSR by a marine sulfate-reducing bacterium, DMSS-1, a *Desulfovibrio* species, isolated from salt marsh in Cape Cod, MA. Submicromolar levels of iron increase sulfur isotope fractionation by about 50% relative to iron-replete cultures of DMSS-1. Iron-limited cultures also exhibit decreased cytochrome *c*-to-total protein ratios and cell-specific sulfate reduction rates (csSRR), implying changes in the electron transport chain that couples carbon and sulfur metabolisms. When DMSS-1 fixes nitrogen in ammonium-deficient medium, it also produces larger fractionation, but it occurs at faster csSRRs than in the ammonium-replete control cultures. The energy and reducing power required for nitrogen fixation may be responsible for the reverse trend between S-isotope fractionation and csSRR in this case. Iron deficiency and nitrogen fixation by sulfate-reducing microbes may lead to the large observed S-isotope effects in some euxinic basins and various anoxic sediments.

Microbial sulfate reduction (MSR) is a process of anaerobic respiration that utilizes sulfate as an electron acceptor. This process remineralizes organic carbon in anoxic marine sediments and is the main driver of the global biogeochemical cycle of sulfur (8, 13). Of the four stable isotopes of sulfur in nature (^{32}S, ^{33}S, ^{34}S, and ^{36}S), MSR preferentially utilizes lighter S-isotopes, producing sulfide that is depleted in heavy isotopes relative to the reactant sulfate. This isotope fractionation between sulfate and sulfide has been widely used to trace the biogeochemical cycling of sulfur and carbon (43, 48). Numerous studies have characterized S-isotope fractionation in pure and mixed cultures of sulfate-reducing microbes, demonstrating a general correlation between sulfate reduction rates and the magnitude of S-isotope fractionation (6 and 62 and references therein). Most of these studies investigated the influence of terminal electron acceptor, sulfate, and electron donors (organic substrates or H_2) on microbial S-isotope fractionation. These studies reported lower fractionations at sulfate concentrations below ~200 μM (14, 27, 28, 32) and attributed higher fractionations to the limitation by organic electron donors or the presence of recalcitrant organic substrates (15, 40, 62, 63). However, links between environmental variables and physiological mechanisms that control sulfate reduction rates within cells deserve further investigation. In particular, sulfate-reducing microbes do not translocate electrons from the organic substrate directly to the terminal electron acceptor, sulfate. Instead, the rates of electron transfer depend on a number of enzymes and electron carriers (41, 54). Thus, any alterations in the electron transfer chain and changes in the flow of energy and reducing equivalents within the cell may ultimately influence the magnitude of S-isotope fractionation by changing the coupling between the electron donor and sulfate.

Importantly, these changes may arise from environmental limitations. For example, iron is a cofactor in many enzymes and electron carriers in microbial electron transfer chains, including hydrogenases, ferredoxin, or cytochromes (54, 58). Consequently, iron deficiency affects the synthesis and function of these enzymes and carriers in various microbes (17, 37), including sulfate-reducing bacteria (55), and likely affects the conservation of respiratory energy (31). The cellular energy and redox budgets also change if some of the reducing equivalents generated by the oxidation of organic substrates are diverted toward metabolic processes such as nitrogen fixation. In addition to the respiratory machinery, limitation of microbial growth by nitrogen is expected to affect general protein synthesis.

Here, we report the effect of Fe and N limitation on the physiology of and S-isotope fractionation by a marine sulfate-reducing bacterium, DMSS-1, a *Desulfovibrio* species, recently isolated from marine sediment (62). Although these two limitations are expected to affect different cellular processes, both influence S-isotope effects. The potential significance of both limitations and their accompanying S-isotope fractionations are discussed in an environmental context. To the best of our knowledge, previous studies have not investigated the effect of iron and other nutrient limitations on S-isotope fractionation during MSR.

MATERIALS AND METHODS

Organism and growth medium. *Desulfovibrio* sp. strain DMSS-1, which is used in this study, was isolated from marine coastal sediments in Cape Cod, MA (62, 63). The nucleotide sequences of 16S rRNA and *dsrAB* genes of DMSS-1 have been deposited in GenBank under accession numbers JF968436 and JF968437, respectively. The culture is available upon request. DMSS-1 was grown in a chemically defined medium in batch culture. This medium consisted of (per liter) the following: $NaHCO_3$, 9 g;

Received 6 June 2012 Accepted 16 September 2012
Published ahead of print 21 September 2012
Address correspondence to Min Sub Sim, mssim@earth.northwestern.edu.
* Present address: Min Sub Sim, Department of Earth and Planetary Sciences, Northwestern University, Evanston, Illinois, USA.

doi:10.1128/AEM.01842-12

TABLE 1 Growth parameters and isotope fractionations in batch cultures containing different concentrations of iron and ammonium[a]

Organic substrate	Concn of:		Growth yield (10^6 cells/μmol sulfate reduced)	csSRR (fmol/cell/day)	Sulfide produced (mM)	Isotopic ratio (‰):		
	NH_4Cl	$FeCl_2$ (μM)				$\delta^{34}S_{sulfate}$	$\delta^{34}S_{sulfide}$	$^{34}\varepsilon$
Lactate	5.6 mM	8	29 ± 5	28.1 ± 2.6	7.4	2.0	−6.4	6.8 ± 0.2
	5.6 mM	8	32 ± 5	25.1 ± 2.5	8.7	3.1	−5.9	7.0 ± 0.2
	5.6 mM	<1	15 ± 2	18.7 ± 1.4	9.3	5.5	−9.9	11.7 ± 0.3
	5.6 mM	<1	18 ± 3	20.1 ± 1.7	8.2	4.8	−8.4	10.4 ± 0.3
	112 μM	8	7 ± 1	62.4 ± 5.2	8.5	3.3	−7.4	8.4 ± 0.3
	56 μM	8	9 ± 1	62.9 ± 5.7	8.6	3.4	−6.7	7.8 ± 0.2
Malate	5.6 mM	8	114 ± 18	5.3 ± 0.7	6.8	5.5	−14.6	16.7 ± 0.3
	5.6 mM	8	94 ± 15	4.9 ± 0.5	6.6	6.6	−16.3	19.1 ± 0.3
	5.6 mM	8	99 ± 16	4.3 ± 0.5	7.5	7.2	−15.9	18.6 ± 0.3
	5.6 mM	2	110 ± 17	4.1 ± 0.4	6.5	5.7	−15.4	17.5 ± 0.3
	5.6 mM	<1	63 ± 10	2.9 ± 0.3	4.6	5.0	−23.4	25.1 ± 0.3
	5.6 mM	<1	66 ± 10	2.2 ± 0.2	3.1	3.4	−27.9	28.9 ± 0.3
	56 μM	8	19 ± 3	6.5 ± 0.7	6.5	7.8	−18.5	21.9 ± 0.4
	5.6 μM	8	16 ± 3	8.3 ± 0.7	6.6	7.8	−19.4	22.6 ± 0.4
	0.5 μM	8	19 ± 3	8.5 ± 0.7	6.9	8.6	−19.0	22.7 ± 0.4

[a] Each row represents a single independent experiment, and errors were propagated from analytic uncertainties of cell density, sulfide, and isotope measurements. Isotopic ratios were reported with respect to the laboratory working reference SF_6.

KH_2PO_4, 0.2 g; NaCl 21g; $MgCl_2 \cdot 6H_2O$, 3 g; KCl, 0.5 g; $CaCl_2 \cdot 2H_2O$, 0.15 g; resazurin, 1 mg; 1 ml of trace element solution SL-10 without $FeCl_2$ (68); 10 ml of vitamin solution described as a part of DSMZ medium 141 (catalogue of strains 1993; DSMZ, Braunschweig, Germany); and 1 ml of selenium stock solution (0.4 mg of Na_2SeO_3 per 200 ml of 0.01 N NaOH). Sodium ascorbate (1 g per liter) was added as a reducing agent. Cultures contained either lactate (20 mM) or malate (18 mM) as electron donors and carbon sources and 21 mM Na_2SO_4 as an electron acceptor. The medium was titrated to pH 7.5 and sterilized anaerobically under 80% N_2-20% CO_2 gas. The background concentration of iron in the basal medium, i.e., the concentration before the addition of iron stock solution, was 0.7 ± 0.2 μM, as measured by inductively coupled plasma-optical emission spectroscopy (ActLab, Ontario, Canada). The background concentration of ammonium in the basal medium before the addition of ammonium stock solution was 0.5 ± 0.2 μM, as measured by a fluorometric method (36). Regular (control) growth medium contained 10 ml of anoxic NH_4Cl stock solution (3 g/100 ml water) and 1 ml of $FeCl_2 \cdot 4H_2O$ stock solution (150 mg $FeCl_2 \cdot 4H_2O$ in 100 ml of 0.25% HCl) per liter with final concentrations of 5.6 mM NH_4Cl and 8 μM $FeCl_2$, respectively. In growth limitation experiments, ammonium and iron stock solutions were serially diluted with anoxic water and 0.25% HCl, respectively, before they were added to the basal medium. The speciation of soluble iron in the medium was calculated at pH 7.5 and at a redox potential lower than −111 mV, as indicated by the conversion of resorufin (pink) to dihydroresorufin (colorless) (39). Calculations show that $FeCO_3^0$ is the dominant form of dissolved iron in both control and iron-limited media and that the precipitation of $Fe(OH)_3(s)$, $FeCO_3(s)$, and $Fe_3(PO_4)_2(s)$ is not to be expected. Indeed, the fresh medium contained no observable precipitate. Concentrations of iron and ammonium used in different experiments are listed in Table 1.

Culture experiments. DMSS-1 was incubated in batch cultures containing different concentrations of iron or ammonium (Table 1). Effects of limitations by iron and ammonium were reproducible and confirmed in multiple independent experiments (Fig. 1 and Table 1). Culture bottles (165 ml) containing sterile media (100 ml) were inoculated with washed cells. The cells were washed three times by anaerobic centrifugation and resuspension in fresh medium that lacked both iron and ammonium to minimize the carryover of sulfide, iron, and ammonium. Growth (optical density, cell counts, and protein) and sulfide concentrations were monitored every day in lactate-grown cultures and every other day in malate-grown cultures. Sulfide concentration was measured by a modified methylene blue assay (16) in 200-μl culture samples fixed by 1 ml of 0.05 M Zn-acetate solution. Growth was monitored by measuring the optical density at 630 nm using a Synergy2 Biotek microplate reader (Biotek, Winooski, VT) and by microscopic counts of cells stained by SYTOX-Green nucleic acid stain (S7020; Invitrogen, Paisley, United Kingdom) using a Zeiss Axio Imager M1 epifluorescence microscope (Carl Zeiss, Thornwood, NY). Microbial activity in cultures was terminated by the addition of 20 ml of 1 M Zn-acetate, and dissolved sulfide was precipitated as zinc sulfide. These samples were stored at 4°C until the extraction of sulfur and the subsequent isotope analysis. Preincubation experiments were conducted to determine the concentrations of sulfide and final cell densities produced under iron- and nitrogen-limited conditions. These cultures and control cultures contained the same amounts of sulfide at the onset of the stationary phase (not shown here).

Nitrogenase activity. Nitrogenase activity was determined in actively growing cultures of DMSS-1 using a modified acetylene reduction technique (21). Acetylene gas (20 ± 1 μmol) was injected into a set of culture bottles containing 10 ml of ammonium-free medium, and the bottles were subsequently inoculated with washed cells. One bottle was sacrificed every 2 days to monitor ethylene production from acetylene. H_2S was removed from the headspace by adding 1 ml of 1 M zinc acetate solution, and 0.5 ml of the headspace gas was withdrawn using a gas-tight syringe. The gas sample was analyzed by a gas chromatograph (Shimadzu GC-2014) equipped with a flame ionization detector and a packed column (60/80 mesh; outer diameter, 1/8 in.; length, 4.6 m; Carboxen, Supelco). Oven temperature was held at 125°C for 5 min, increased to 225°C at a rate of 20°C/min, and held at 225°C for 5 min. Procedural and analytical reproducibility was 8%. Ethylene production was monitored in parallel control sterile media and cultures, both containing 5.6 mM ammonium.

Cytochrome spectra. Reduced and oxidized cytochrome spectra and the differences between the two were obtained using the whole-cell method (37, 38). Cells were harvested from 45 ml of the culture by centrifugation at 3,000 × *g* for 15 min. The supernatant was discarded, and the cells were resuspended in 1 ml of phosphate-buffered saline solution (PBS; 50 mM phosphate buffer and 350 mM NaCl). Cell suspensions were transferred into 1.5-ml microcentrifuge tubes, washed twice by centrifugation (13,000 × *g*, 3 min), and resuspended in PBS. Protein was determined using a Pierce bicinchoninic acid protein assay kit (Pierce, Rockford, IL) with an albumin standard, and the cells were resuspended in PBS at ~1.5 mg protein/ml. The resuspended cultures were transferred into flat-bottom 96-well plates (200 μl well volume) and oxidized or reduced

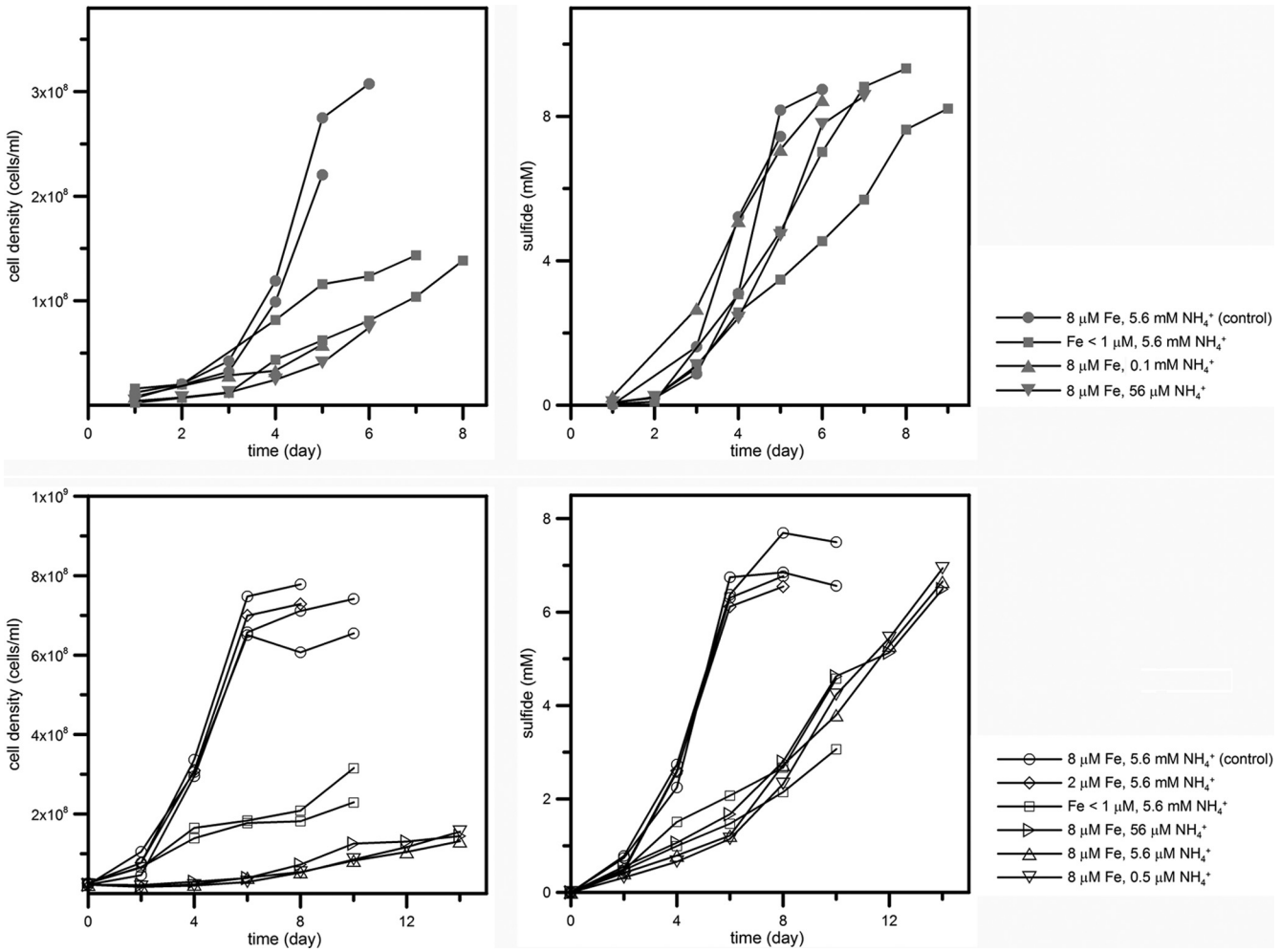

FIG 1 Effect of iron and ammonium limitation on growth (left) and sulfide production (right) of DMSS-1 grown on lactate (upper) and malate (lower). Each line indicates a single independent experiment. Both control and nutrient-limited cultures produced similar amounts of sulfide at the end of the incubation, indicating that iron and nitrogen limitation caused a reduction of overall growth rate and not an extended lag phase followed by the same growth rate. For malate-grown iron-limited cultures, the incubation was stopped before the cessation of growth (see Materials and Methods). Concentrations of iron and ammonium were estimated at the beginning of the incubation. Cell density is subject to a ±15% error, and the analytical uncertainty of the measurement of sulfide concentrations is ±5%.

by the addition of 20 μl of 30% H_2O_2 and 20 μl of freshly prepared 50 mg/ml sodium dithionite stock solution, respectively. After a 1-min incubation at room temperature, the cells were shaken in the Synergy2 microplate reader (BioTek, Winooski, VT) for 10 s, and optical absorption between 400 and 700 nm was measured in 2-nm intervals.

Isotope measurements. Sulfide was extracted by acidifying the culture medium with 6 N HCl at 80°C under a flow of nitrogen gas for 2 h. Sulfide produced during the distillation was precipitated as ZnS in a Zn-acetate solution (0.18 M). After the extraction of sulfide, sulfate in the remaining medium was reduced to sulfide with 30 ml of the reducing agent (mixture of HI, H_3PO_2, and HCl) (66). Samples were boiled and purged by N_2 gas for 2 h. Volatile products were passed through a condenser and a trap containing distilled water, and sulfide was subsequently collected in a Zn-acetate trap. ZnS was converted to Ag_2S by the addition of $AgNO_3$ and incubation at 70°C for 1 day. Ag_2S was centrifuged, washed with distilled water three times, and dried at 70°C. The Ag_2S samples reacted with an excess of fluorine gas for more than 5 h at 300°C, and the produced SF_6 was purified by gas chromatography. Purified SF_6 was transferred into an isotope-ratio mass spectrometer for sulfur isotope measurements in dual inlet mode (52).

Data processing. Cellular growth yield during the vegetative phase was calculated as the ratio of the increase in the number of cells and the amount of sulfide produced during the experiment. Because growth in iron- and ammonium-limited cultures was not exponential, the average cell-specific sulfate reduction rates (csSRR) during the vegetative phase were calculated as

$$\mathrm{csSRR} = \frac{[H_2S]_N - [H_2S]_1}{\sum_{n=1}^{N-1} \frac{C_n + C_{n+1}}{2} \cdot (t_{n+1} - t_n)} \quad (1)$$

where $[H_2S]_1$ and $[H_2S]_N$ are sulfide concentrations at the first and the Nth sampling times, t_n is the time of sampling, and C_n is the cell density at each sampling point. In previous studies, csSRR was calculated using the cell densities at two time points (20), but equation 1 used more cell density data to reflect growth more realistically. The form of equation 1 is the same as the one used in previous studies (20) if N is set to 2.

The isotope fractionation factor (α) in the batch culture experiment was calculated using the modified Rayleigh distillation equation as previously described (62):

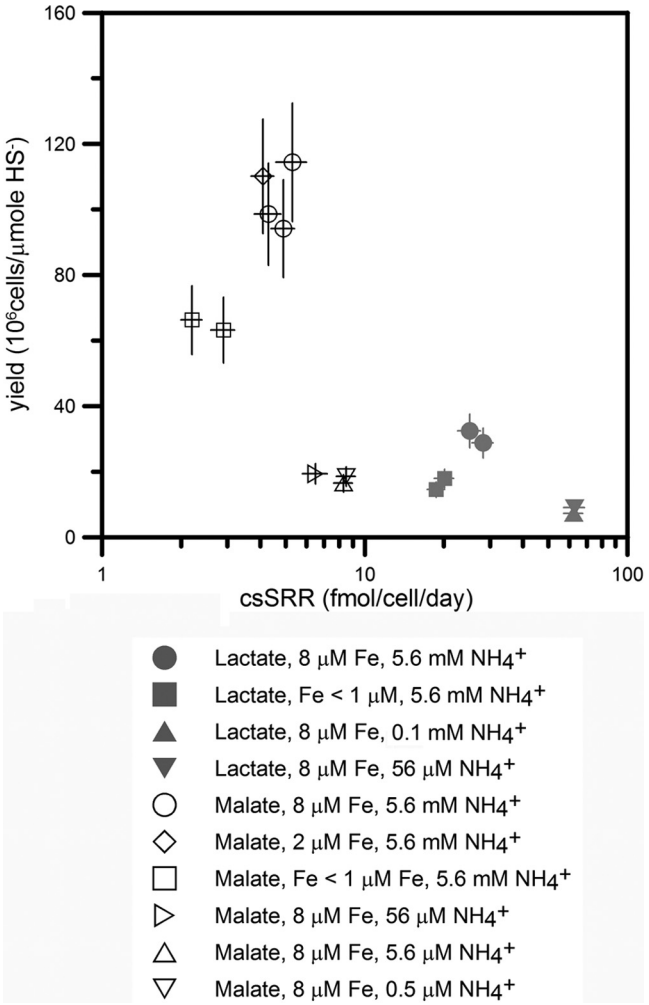

FIG 2 Effect of iron and ammonium limitation on DMSS-1 growth yields and cell-specific sulfate reduction rate (csSRR). Both limitations reduced the growth yield. Iron deficiency decreased csSRR, while cells limited by ammonium respired faster than control cultures. Errors were propagated from analytic uncertainties of cell density and sulfide measurements.

$$^{34}\alpha = -\frac{1}{\ln f_r}\ln\left(1 + \frac{(1 - f_r)}{f_r}\frac{\delta_p + 1{,}000}{\delta_r + 1{,}000}\right) \quad (2)$$

where f_r is the fraction of the remaining sulfate and δ_r and δ_p are sulfur isotope compositions of the remaining sulfate and produced sulfide, respectively. The isotope enrichment factor is defined as

$$^{34}\varepsilon = 1{,}000 \cdot (1 - {}^{34}\alpha) \quad (3)$$

In this definition, positive values represent the depletion of heavy isotopes in the product. For each calculation, errors from cell counts (±15%), sulfide concentration measurements (±5%), and isotope analyses (0.2‰ for $\delta^{34}S$) (51) were propagated according to Bevington and Robinson (5).

Nucleotide sequence accession numbers. The nucleotide sequences of 16S rRNA and *dsrAB* genes of DMSS-1 have been deposited in GenBank under accession numbers JF968436 and JF968437, respectively.

RESULTS

DMSS-1 cultures grew and produced sulfide more slowly in the presence of <1 μM iron and <0.1 mM ammonium than iron- and ammonium-replete cultures (8 μM and 5.6 mM for iron and ammonium, respectively) (Fig. 1 and Table 1). These effects of iron and ammonium limitation could be observed in cultures that used either malate or lactate as the electron donor (Fig. 1 and 2). When cells grew on lactate, reduced concentrations of iron and ammonium reduced the cellular yield to one-half and one-fourth, respectively, relative to the control cultures (Fig. 2 and Table 1). Therefore, concentrations of iron and ammonium lower than 1 μM and 0.1 mM, respectively, limited the growth of DMSS-1. Cell-specific sulfate reduction rates (csSRRs) were lower in iron-limited cultures (19 to 20 fmol/cell/day) but higher in ammonium-limited cultures (62 to 63 fmol/cell/day) relative to the control cultures (25 to 28 fmol/cell/day) (Fig. 2 and Table 1) ($P < 0.05$). When DMSS-1 utilized malate as an electron donor for sulfate reduction, it attained higher cell densities (62) but exhibited slower csSRRs than during sulfate reduction coupled with the oxidation of lactate (Fig. 2 and Table 1). Iron limitation in malate-fed cultures diminished both the growth yield and the csSRR compared to the malate-fed control cultures ($P < 0.05$). Limitation by ammonium reduced the growth yield to 20% of the control cultures while accelerating the cell-specific respiration rate (Fig. 2 and Table 1).

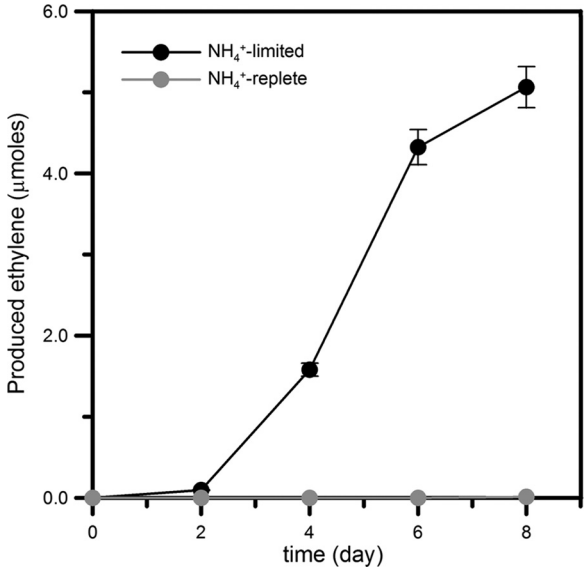

FIG 3 Production of ethylene by the reduction of acetylene in ammonium-limited medium (0.5 μM ammonium). Ethylene was not detected (<10 nmol) in cultures that contain 5.6 mM ammonium. Error bars indicate procedural and analytical reproducibility (±8%).

The growth of DMSS-1 in ammonium-limited medium suggested that this organism could fix nitrogen and use it in biosynthesis. Indeed, ammonium-limited cultures produced ethylene by acetylene reduction, but ethylene was not detected in ammonium-replete cultures and sterile controls (Fig. 3).

A slower respiration rate by DMSS-1 in iron-limited cultures indicated that this metal was impairing the function of respiratory proteins, among other processes. To test this further, we examined how iron limitation affected the content of cytochrome *c*, one of the essential proteins in electron transfer chains. Reduced minus oxidized spectra of iron-replete cells showed predominant peaks at 420 to 422, 523 to 524, and 552 to 553 nm, typical for *c*-type cytochromes (Fig. 4) (55, 57). These peaks were more than twice as large in cells cultured in the iron-replete medium than in the iron-limited medium (Fig. 4). Therefore, the abundance of cyto-

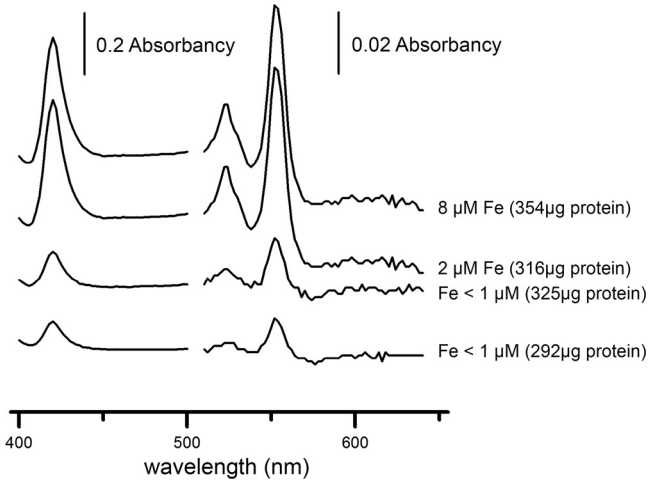

FIG 4 Reduced minus oxidized spectra of whole cells of DMSS-1 grown in media containing 18 mM malate, 5.4 mM ammonium, and different concentrations of iron. Three peaks typical for the absorption by cytochrome *c* were prominent in iron-replete cells. The ratios of these peaks to the background signal were smaller when DMSS-1 was grown in iron-deficient media. All samples contained similar amounts of total protein (values stated in the brackets).

chrome *c* (per cell protein) was lower in iron-limited cultures than in iron-replete cultures.

Analyses of S-isotope ratios of sulfates and sulfides in DMSS-1 cultures limited by iron or ammonium showed that both limitations increased the magnitude of sulfur isotope fractionation (Table 1). The calculated enrichment factor ($^{34}\varepsilon$) in control cultures grown on lactate was 6.9‰ ± 0.2‰ (averages ± standard errors of the means; $n = 2$), as previously reported (62). Iron-deficient cells grown on lactate fractionated $^{34}S/^{32}S$ up to 12‰, while limitation by ammonium increased the enrichment factors in lactate-grown cultures by only 1‰ with respect to the control cultures (Fig. 5 and Table 1). Overall, larger fractionation factors associated with the growth on malate amplified the isotopic effects of limitations by iron and ammonium. Malate-fed, iron- and ammonium-replete cultures fractionated ^{34}S at 18‰ ± 1‰ (averages ± SEM; $n = 3$), while limitations by ammonium and iron increased this enrichment factor to 23 and 29‰, respectively (Fig. 5 and Table 1).

DISCUSSION

Iron limitation. At the end of the incubation experiments using lactate-grown cultures, sulfide concentration increased up to 8.5 mM. Our calculations indicate that in the presence of high concentrations of sulfide, most of the dissolved iron forms complexes (e.g., $FeHS^+$) (60). Under these conditions, the concentration of free ferrous ion is around 3 nM and 0.3 nM in control and iron-limited media, respectively. The corresponding ion activity product (IAP) values ($[Fe^{2+}][HS^-]/[H^+]$) in control and iron-limited media are $10^{-2.9}$ and $10^{-3.9}$, respectively. These values are comparable to the equilibrium solubility products of amorphous FeS ($10^{-2.95}$) and mackinawite ($10^{-3.6}$) (18). Iron in the form of amorphous FeS is considered to be bioavailable (e.g., see reference 30). The media should be supersaturated with respect to pyrrhotite and pyrite (18), but the precipitation of these crystalline sulfides requires longer incubation times than those used in our study (33). More importantly, DMSS-1 grew slower and fractionated more in media that initially contained less iron than in control cultures. Hence, the contrast between control and iron-limited cultures can be attributed to different availabilities of iron regardless of the precipitation of poorly crystalline iron sulfide minerals.

Iron deficiency reduced the growth rate and cell-specific sulfate reduction rate (csSRR) of DMSS-1 and led to increasing fractionation factors. This inverse relationship between csSRR and $^{34}\varepsilon$ was previously reported for DMSS-1 cultures that grew in the presence

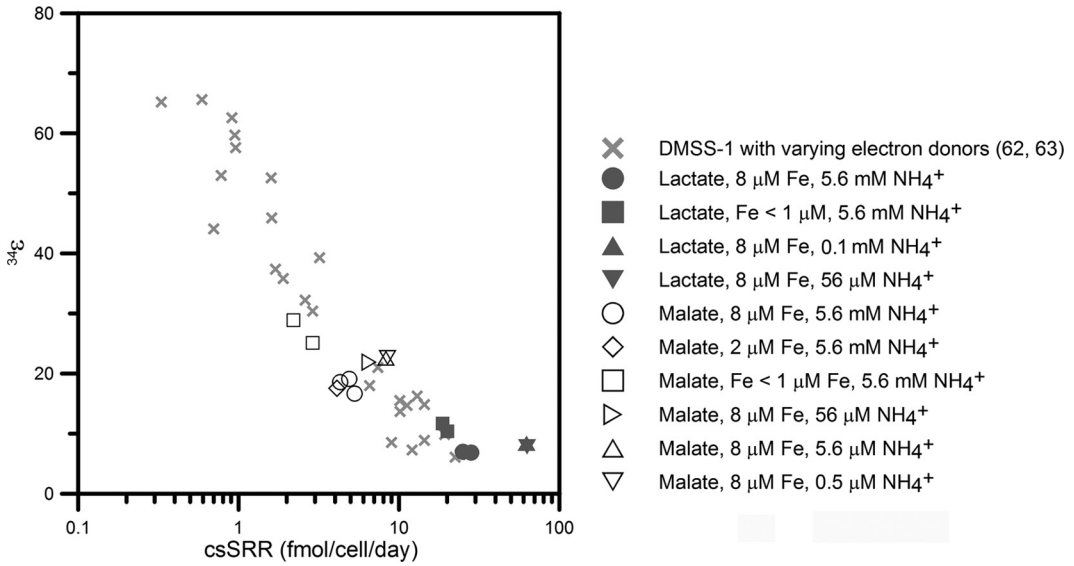

FIG 5 Variations in $^{34}\varepsilon$ and cell-specific sulfate reduction rate (csSRR) in DMSS-1 cultures limited by iron or ammonium (this study) or various electron donors (62, 63). Iron deficiency reduced csSRR and led to increasing fractionation factors. A similar relationship between csSRR and $^{34}\varepsilon$ is observed when the csSRR rates in DMSS-1 are changed by changing the concentration of a single electron donor or changing the type of organic electron donor (62, 63). In contrast, nitrogen limitation increased both csSRR and $^{34}\varepsilon$.

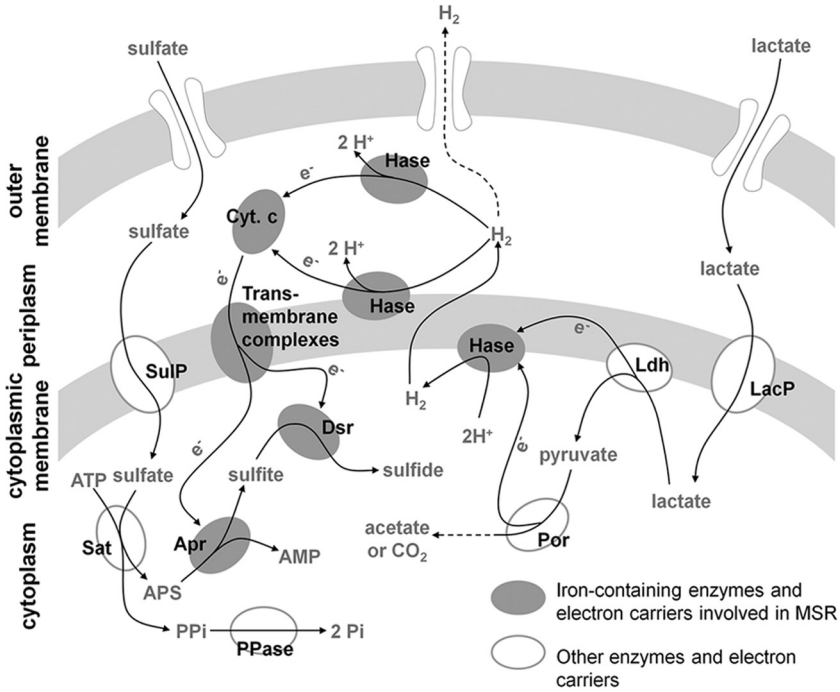

FIG 6 Schematic representation of electron flow during MSR through hydrogen cycling in Gram-negative sulfate-reducing bacteria that oxidize lactate (41, 49, 54). Malate is also oxidized via pyruvate, but the transfer of reducing equivalents from the first oxidation step of malate may differ from that of lactate oxidation (44). Many enzymes and electron carriers involved in this process, from the cytoplasm to the periplasm, contain iron in their active sites (45, 58). Iron limitation impairs the synthesis of cytochromes and hydrogenases (55), reducing the flow of electrons to the sulfate reduction system. Abbreviations: LacP, lactate permease; Ldh, lactate dehydrogenase; Por, pyruvate-ferredoxin oxidoreductase; Hase, hydrogenase; Cyt. *c*, cytochrome *c*; SulP, sulfate permease; Sat, ATP sulfurylase; Apr, APS reductase; Dsr, dissimilatory sulfite reductase; PPase, pyrophosphate phosphatase.

of different electron donors (Fig. 5) (62) but were not limited by nitrogen or iron. The similarities between the effects of organic limitation and iron on the relationship between csSRR and $^{34}\varepsilon$ are consistent with a central role of iron in the MSR pathway, given that both iron and electron donors can dictate the rate at which electrons are supplied to the sulfate reduction system (9, 62, 63). In contrast to previous reports, which considered the effect of electron donors and acceptors on the relationship between csSRR and $^{34}\varepsilon$ (15, 28, 32, 40, 62), to the best of our knowledge, this is the first study that considers the effect of other limitations on S isotope fractionation by a sulfate-reducing microbe.

Although the mechanism of energy conservation by sulfate-reducing bacteria is not fully understood, H_2 cycling between cytoplasm and periplasm is thought to be involved in this process (Fig. 6) (49). In the H_2-cycling model, electrons generated by the oxidation of organic compounds react with protons to form H_2 in reactions catalyzed by various Fe-containing cytoplasmic hydrogenases. H_2 then diffuses across the cytoplasmic membrane into the periplasm, where it is split into protons and electrons by periplasmic hydrogenases. Electrons return to the cytoplasm through cytochromes and transmembrane protein complexes and are delivered to terminal reductases and used to reduce sulfate. The protons remaining in periplasm generate proton motive force. This model requires both cytoplasmic and periplasmic hydrogenases, enzymes that invariably contain iron in their active site (54). The key electron carrier involved in H_2 cycling, a cytochrome *c*, is also a metalloprotein containing a heme prosthetic group (55). Increasing genetic and biochemical evidence points to the presence of redundant electron transport chains, suggesting that hydrogen cycling is not essential for the energy conservation in sulfate-reducing bacteria (41). Nonetheless, because most components involved in alternative electron transport pathways contain iron in their active sites (54), iron limitation would conceivably affect the function of electron transfer pathways. Our experiments strongly support a role of iron in the electron transfer chain that couples sulfate reduction and oxidation of lactate or malate in DMSS-1 cells. In particular, the ratio of cytochrome *c* to total protein decreases in iron-starved DMSS-1 cells (Fig. 4). This decrease likely impairs the flow of electrons from organic electron donors to sulfur through H_2 cycling and slows down the respiration. This measurable effect is one of the many potential changes in the activities and concentrations of components involved in MSR during iron limitation. These changes can be explored by future transcriptomic, proteomic, and biochemical studies.

The reduced flow of electrons to the sulfate reducing system would affect S-isotope fractionation. According to the reaction and isotope fractionation scheme for MSR initially developed by Rees (59) and further modified by Brunner and Bernasconi (9) and Farquhar et al. (23) (referred to as the RBF model), the MSR pathway consists of several enzymatic steps that are thought to be reversible. These reversible steps include ATP sulfurylation, reduction of adenosine-5′-phosphosulfate (APS), and reduction of sulfite. The RBF model explains the overall S-isotope fractionation by considering both the intrinsic isotope effects of these enzymatic steps and the ratios between forward and backward fluxes (reversibility) at each step, predicting the increase in S-isotope fractionation when reversibilities approach unity. Isotope effects at individual enzymatic steps depend on the difference be-

tween ground-state and transition-state structures in each reaction (50) and are unlikely to be altered by nutrient availability. Instead, larger S-isotope effects in iron-limited cultures suggest MSR operating in a more reversible manner. Given that electrons are essential for sulfate reduction, a slower flow of electrons to terminal reductases could slow down the forward reactions and increase the reversibility, thereby increasing the overall isotope fractionation. Our results suggest that this slowing down can be triggered by a deficiency in iron-dependent components of the respiratory chain. Limitations by other metals required for MSR, such as Co, Zn, Ni, and Se (25, 54), on S-isotope effects remain to be explored in future studies.

Ammonium limitation. Acetylene reduction assay confirms that DMSS-1 can fix nitrogen in ammonium-limited media (Fig. 3), an ability that DMSS-1 shares with other *Desulfovibrio* species (56). Nitrogen limitation diminishes the growth yield of DMSS-1 in spite of increased csSRR (Fig. 2). The higher respiratory rates likely support the energetically costly N_2 fixation, a process that requires 8 electrons and 16 ATP molecules (56). In other words, if a larger portion of energy generated by the respiratory activity is spent on nitrogen fixation rather than biosynthesis, the growth yield decreases. Unlike the limitation by iron or organic compounds, which decreased csSRR and increased $^{34}\varepsilon$, nitrogen limitation increased both csSRR and $^{34}\varepsilon$ in DMSS-1 cultures (Fig. 5). The RBF model described above ascribes the overall isotope fractionation during MSR to the reversibility and the intrinsic isotope effect of each enzymatic step, predicting that MSR operates in a more reversible manner during diazotrophic growth of DMSS-1. At this point, it is unclear how this model prediction can account for the intracellular physiology, given that N_2 fixation acts as a sink for reducing power but the csSRR is higher. In other words, N_2 fixation should draw electrons out of the MSR pathway, increasing S-isotope fractionation, but the higher csSRR reflects the increased net flow of electrons through the MSR pathway during diazotrophic growth of DMSS-1.

Interestingly, both iron- and ammonium-limited cultures of DMSS-1 exhibit slow and nonexponential growth kinetics, consistent with the density-dependent limitation by a substrate that is present in the initial medium (69). Not only are cell densities at the end of growth lower than those in iron- and ammonium-replete cultures but the growth rates are also much slower, suggesting different growth physiologies in these cultures. These differences between nutrient-limited and nutrient-replete cultures cannot be attributed to the production of observable extracellular polymers, cell clumping, or measurable changes in cell size. Instead, relevant examples of similar, slow growth kinetics occur in cultures of syntrophic organisms limited by energy supply (22) and microbes that produce intracellular granules (53). Namely, both nitrogen fixation and the lack of iron in critical energy-generating enzymes are expected to reduce the energy yield available for biosynthesis of new cellular material and cell doubling. In the presence of abundant carbon and reducing equivalents, these limitations can promote the formation of intracellular polyglucose granules at the expense of other cellular material. The link between low iron and ammonium availability and the synthesis of abundant intracellular polyglucose granules is observed in various *Desulfovibrio* species and *Desulfobulbus propionicus* (64). In addition, given that nitrogenases contain an iron cofactor (10), iron limitation can aggravate the effects of nitrogen limitation in nature. One could expect larger fractionations in the media that contain low concentrations of iron and nitrogen, although our experiments did not directly test this possibility.

Environmental and geological significance. Effects of iron and nitrogen limitation on S-isotope fractionation can inform interpretations of sulfur isotope data in modern and ancient environments. Porewaters in the natural habitat of DMSS-1, salt marsh sediments, are characterized by dissolved Fe concentrations that range from 2 to 60 μM (26), i.e., they are higher than the submicromolar iron concentrations limiting the growth of DMSS-1 under our experimental conditions. It is thus unlikely that these bacteria are limited by iron in their natural habitat. In the oxic water column, iron oxyhydroxides accumulate in the oxic surface sediment and are subsequently reduced and dissolved during early diagenesis. Consequently, in most marine environments, the concentration of dissolved iron (II) in the porewaters of the sulfate reduction zone is usually several to several hundred μM (7, 35, 42, 67). Under these conditions, iron is not the key factor controlling the magnitude of microbial S-isotope fractionation in the subsurface zone of sulfate reduction. However, the situation may be different in euxinic basins, where iron oxyhydroxides dissolve and form FeS and pyrite while settling through a sulfidic water column (11). For example, in the euxinic part of the Black Sea, iron concentrations are usually lower than 0.3 μM in the water column (2, 46) and lower than 1 μM in the porewater (11). The submicromolar concentrations of dissolved iron may limit MSR and contribute to the production of sulfides depleted up to 60‰ (65). The same mechanism may have been relevant in the past, particularly during times of oceanic euxinia when sulfidic conditions would have expanded from subsurface sediments into the water column (47). This expansion, accompanying the syngenetic formation of pyrite in the water column (34), might have diminished the overall availability of iron for marine sulfate-reducing microbes, thereby increasing the magnitude of S-isotope fractionation. This hypothesis may explain some of the >20‰ increase in S-isotopic difference between sedimentary sulfide and sulfate at the onset of the Cretaceous Oceanic Anoxic Event 2 (1, 34).

By exploring the effect of N_2 fixation on S-isotope fractionation by sulfate reducers, our observations indicate that nitrogen limitation increase the already large S-isotope fractionation in areas characterized by low productivity, such as deep sea sediments (e.g., see reference 61). Organic compounds limit the growth and MSR in these settings, but the nitrogen requirement of microbial communities in deep sea sediments may further increase $^{34}\varepsilon$ depending on the C/N ratio of organic substrates used for growth (3). More surprisingly, recent studies also have correlated nitrogen fixation with the activity of sulfate reducers in porewaters characterized by ammonium concentrations as high as 1 mM (4) and in organic-rich estuarine sediments (24). Nitrogen fixation thus occurs in sediments under hypoxic water columns even though the porewater ammonium concentrations are higher than 0.1 mM (4). These concentrations are comparable to those limiting the growth of DMSS-1 in our laboratory cultures (Fig. 1). Nitrogen fixation by sulfate reducers in organic-rich areas and its isotopic signatures have yet to be explored in detail, but our data predict higher S-isotope fractionations even in zones with rather high rates of sulfate reduction if sulfate reducers also fix N_2. These conditions may be met in various estuarine sediments (24), oxygen minimum zones, hypoxic fjords (4), and, possibly, in Lake Cadagno, a meromictic lake in Switzerland. In this lake, dense

populations of anoxygenic phototrophic bacteria at the chemocline enrich the underlying monimolimnion and sediments with organic compounds accessible to sulfate-reducing microbes (19), and sulfate-reducing *Deltaproteobacteria* there fix N_2 (29), likely contributing to a portion of the S-isotope difference between dissolved sulfate and sulfide, which is often as large as 45‰ (12). These hypotheses can be tested experimentally by parallel measurements of the expression of nitrogenases, sulfate-reducing rates, and S-isotope fractionations.

Emerging constraints on the physiological coupling among S, C, Fe, N, and other cycles show that controls on natural S-isotope signatures are complex and may involve limitations by various nutrients. In particular, the effects of iron and nitrogen on S-isotope fractionation described by this study underscore the need to better understand nutrient and metal requirements of sulfate-reducing microbes in natural settings. While this may complicate current interpretations of the S-isotope record, it will also draw more realistic and better informed links between microbial physiology and sedimentary biogeochemistry.

ACKNOWLEDGMENTS

This work was supported by grants from the NASA Astrobiology Institute and NSF (EAR-1159318) to S.O. and T.B.

We are grateful to all members of our laboratory for their support. We thank the four anonymous reviewers for constructive suggestions that improved the manuscript.

REFERENCES

1. **Adams DD, Hurtgen MT, Sageman BB.** 2010. Volcanic triggering of a biogeochemical cascade during Oceanic Anoxic Event 2. Nat. Geosci. **3**:201–204.
2. **Alkan N, Tüfekçi M.** 2009. Distribution of dissolved forms of manganese and iron in the water column of the southeastern Black Sea. Turk. J. Fish. Aquat. Sci. **9**:159–164.
3. **Anderson TR, Pondaven P.** 2003. Non-redfield carbon and nitrogen cycling in the Sargasso Sea: pelagic imbalance and export flux. Deep Sea Res. I **50**:573–591.
4. **Bertics VJ, et al.** 2012. Occurrence of benthic microbial nitrogen fixation coupled to sulfate reduction in the seasonally hypoxic Eckernförde Bay, Baltic Sea. Biogeosciences **9**:6489–6533.
5. **Bevington PR, Robinson DK.** 2003. Data reduction and error analysis for the physical sciences, 3rd ed. McGraw-Hill, New York, NY.
6. **Bolliger C, Schroth MH, Bernasconi SM, Kleikemper J, Zeyer J.** 2001. Sulfur isotope fractionation during microbial sulfate reduction by toluene-degrading bacteria. Geochim. Cosmochim. Acta **19**:3289–3298.
7. **Böttcher ME, et al.** 2000. The biochemistry, stable isotope geochemistry, and microbial community structure of a temperate intertidal mudflat: an integrated study. Cont. Shelf Res. **20**:1749–1769.
8. **Bottrell SH, Newton R.** 2006. Reconstruction of change in global sulfur cycling from marine sulfate isotopes. Earth Sci. Rev. **75**:59–83.
9. **Brunner B, Bernasconi SM.** 2005. A revised isotope fractionation model for dissimilatory sulfate reduction in sulfate reducing bacteria. Geochim. Cosmochim. Acta **69**:4759–4771.
10. **Burgess BK.** 1990. The iron-molybdenum cofactor of nitrogenase. Chem. Rev. **90**:1377–1406.
11. **Calvert SE, Karlin RE.** 1991. Relationships between sulphur, organic carbon, and iron in the modern sediments of the Black Sea. Geochim. Cosmochim. Acta **55**:2483–2490.
12. **Canfield DE, Farquhar J, Zerkle AL.** 2010. High isotope fractionations during sulfate reduction in a low-sulfate euxinic ocean analog. Geology **38**:415–418.
13. **Canfield DE, Raiswell R.** 1999. The evolution of the sulfur cycle. Am. J. Sci. **299**:679–723.
14. **Chambers LA, Trudinger PA.** 1979. Microbiological fractionation of stable sulfur isotopes: a review and critique. Geomicrobiol. J. **1**:249–293.
15. **Chambers LA, Trudinger PA, Smith JW, Burns MS.** 1975. Fractionation of sulfur isotopes by continuous cultures of *Desulfovibrio desulfuricans.* Can. J. Microbiol. **21**:1602–1607.
16. **Cline JD.** 1969. Spectrophotometric determination of hydrogen sulfide in natural water. Limnol. Oceanogr. **14**:454–458.
17. **Cotter PA, Darie S, Gunsalus RP.** 1992. The effect of iron limitation on expression of the aerobic and anaerobic electron transport pathway genes in *Escherichia coli.* FEMS Microbiol. Lett. **79**:227–232.
18. **Davison W.** 1991. The solubility of iron sulphides in synthetic and natural water at ambient temperature. Aquat. Sci. **53**:309–329.
19. **Del Don C, Hanselmann KW, Peduzzi R, Bachofen R.** 2001. The meromictic alpine Lake Cadagno: orographical and biochemical description. Aquat. Sci. **63**:70–90.
20. **Detmers J, Bruchert V, Habicht K, Kuever J.** 2001. Diversity of sulfur isotope fractionations by sulfate reducing prokaryotes. Appl. Environ. Microbiol. **67**:888–894.
21. **Dilworth MJ.** 1966. Acetylene reduction by nitrogen-fixing preparations from *Clostridium pasteurianum.* Biochim. Biophys. Acta **127**:285–294.
22. **Dwyer DF, Weeg-Aerssens E, Shelton DR, Tiedje JM.** 1988. Bioenergetic conditions of butyrate metabolism by a syntrophic, anaerobic bacterium in coculture with hydrogen-oxidizing methanogenic and sulfidogenic bacteria. Appl. Environ. Microbiol. **54**:1354–1359.
23. **Farquhar J, et al.** 2003. Multiple sulphur isotopic interpretations of biosynthetic pathways: implications for biological signatures in the sulphur isotope record. Geobiology **1**:27–36.
24. **Fulweiler RW, Nixon SW, Buckley BA, Granger SL.** 2007. Reversal of the net dinitrogen gas flux in coastal marine sediments. Nature **448**:180–182.
25. **Gavel OY, et al.** 1998. ATP sulfurylases from sulfate-reducing bacteria of the genus *Desulfovibrio.* A novel metalloprotein containing cobalt and zinc. Biochemistry **37**:16225–16232.
26. **Giblin AE, Howarth RW.** 1984. Porewater evidence for a dynamic sedimentary iron cycle in salt marshes. Limnol. Oceanogr. **29**:47–63.
27. **Habicht KS, Gabe M, Thamdrup B, Berg P, Canfield DE.** 2002. Calibration of sulfate levels in the Archean ocean. Science **298**:2372–2374.
28. **Habicht KS, Salling L, Thamdrup B, Canfield DE.** 2005. Effect of low sulfate concentrations on lactate oxidation and isotope fractionation during sulfate reduction by *Archaeoglobus fulgidus* strain Z. Appl. Environ. Microbiol. **71**:3770–3777.
29. **Halm H, et al.** 2009. Co-occurrence of denitrification and nitrogen fixation in a meromictic lake, Lake Cadagno (Switzerland). Environ. Microbiol. **11**:1945–1958.
30. **Handley KH, Boothman C, Mills RA, Pancost RD, Lloyd JR.** 2010. Functional diversity of bacteria in a ferruginous hydrothermal sediment. ISME J. **4**:1193–1205.
31. **Harder W, Dijkhuizen L.** 1983. Physiological responses to nutrient limitation. Annu. Rev. Microbiol. **37**:1–23.
32. **Harrison AG, Thode HG.** 1958. Mechanism of the bacterial reduction of sulphate from isotope fractionation studies. Trans. Faraday Soc. **54**:84–92.
33. **Herbert RB, Jr, Benner SG, Pratt AR, Blowes DW.** 1998. Surface chemistry and morphology of poorly crystalline iron sulfides precipitated in media containing sulfate-reducing bacteria. Chem. Geol. **144**:87–97.
34. **Hetzel A, Böttcher ME, Wortmann UG, Brumsack H-J.** 2009. Paleoredox conditions during OAE2 reflected in Demerara Rise sediment geochemistry (ODP Leg 207). Palaeogeogr. Palaeoclimatol. Palaeoecol. **273**:302–328.
35. **Hines ME, Bazylinski DA, Tugel JB, Lyons WB.** 1991. Anaerobic microbial biogeochemistry in sediments from two basins in the Gulf of Maine: evidence for iron and manganese reduction. Estuar. Coast. Shelf Sci. **32**:313–324.
36. **Holmes RM, Aminot A, Kerouel R, Hooker BA, Peterson BJ.** 1999. A simple and precise method for measuring ammonium in marine and fresh water ecosystems. Can. J. Fish. Aquat. Sci. **56**:1801–1808.
37. **Hubbard JAM, Lewandowska KB, Hughes MN, Poole RK.** 1986. Effects of iron-limitation of *Escherichia coli* on growth, the respiratory chains and gallium uptake. Arch. Microbiol. **146**:80–86.
38. **Johnston WA, Huang W, de Voss JJ, Hayes MA, Gillam EM.** 2008. Quantitative whole-cell cytochrome P450 measurement suitable for high-throughput application. J. Biomol. Screen. **13**:135–141.
39. **Jones GA, Pickard MD.** 1980. Effect of titanium (III) citrate as reducing agent on growth of rumen bacteria. Appl. Environ. Microbiol. **39**:1144–1147.
40. **Kaplan IR, Rittenberg SC.** 1964. Microbiological fractionation of sulphur isotopes. J. Gen. Microbiol. **34**:195–212.
41. **Keller KL, Wall JD.** 2011. Genetics and molecular biology of the electron flow for sulfate respiration in *Desulfovibrio.* Front. Microbiol. **2**:135.

42. **King GM, Klug MJ, Wiegert RG, Chalmers AG.** 1982. Relation of soil water movement and sulfide concentration to *Spartina alterniflora* production in a Georgia salt marsh. Science **218**:61–63.
43. **Kleikemper J, et al.** 2002. Activity and diversity of sulfate-reducing bacteria in a petroleum hydrocarbon-contaminated aquifer. Appl. Environ. Microbiol. **68**:1516–1523.
44. **Kremer DR, Nienhuis-Kuiper HE, Timmer CJ, Hansen TA.** 1989. Catabolism of malate and related dicarboxylic acids in various *Desulfovibrio* strains and the involvement of an oxygen-labile NADPH dehydrogenase. Arch. Microbiol. **151**:34–39.
45. **Lamperia J, Pereira AS, Moura JJG.** 1994. Adenylylsulfate reductase from sulfate-reducing bacteria. Methods Enzymol. **243**:241–260.
46. **Lewis BL, Landing WM.** 1991. The biogeochemistry of manganese and iron in the Black Sea. Deep Sea Res. **38**:S773–S803.
47. **Meyer KM, Kump LR.** 2008. Oceanic euxinia in Earth history: causes and consequences. Annu. Rev. Earth Planet. Sci. **36**:251–288.
48. **Moreau JW, Zierenberg RA, Banfield JF.** 2010. Diversity of dissimilatory sulfate reductase genes (*dsrAB*) in a salt marsh impacted by long-term acid mine drainage. Appl. Environ. Microbiol. **76**:4819–4828.
49. **Odom JM, Peck HD, Jr.** 1981. Hydrogen cycling as a general mechanism for energy coupling in the sulfate reducing bacteria, *Desulfovibrio* sp. FEMS Microbiol. Lett. **12**:47–50.
50. **O'Leary MH.** 1989. Multiple isotope effects on enzyme-catalyzed reactions. Annu. Rev. Biochem. **58**:377–401.
51. **Ono S, Keller NS, Rouxel O, Alt J.** 2012. Sulfur-33 consstraints on the origin of secondary pyrite in altered oceanic basement. Geochim. Cosmochim. Acta **87**:323–340.
52. **Ono S, Wing B, Rumble D, Farquhar J.** 2006. High precision analysis of all four stable isotope of sulfur (^{32}S, ^{33}S, ^{34}S and ^{36}S) at nanomole levels using a laser fluorination isotope-ratio-monitoring gas chromatography-mass spectrometry. Chem. Geol. **225**:30–39.
53. **Pagni M, Beffa T, Isch C, Aragno M.** 1992. Linear growth and poly (β-hydroxybutyrate) synthesis in response to pulse-wise addition of the growth-limiting substrate to steady-state heterotrophic continuous cultures of *Aquaspirillum autotrophicum.* J. Gen. Microbiol. **138**:429–436.
54. **Pereira IAC, et al.** 2011. A comparative genomic analysis of energy metabolism in sulfate reducing bacteria and archaea. Front. Microbiol. **2**:69.
55. **Postgate JR.** 1956. Iron and synthesis of cytochrome c_3. J. Gen. Microbiol. **15**:186–193.
56. **Postgate JR.** 1982. The fundamental of nitrogen fixation. Cambridge University Press, Cambridge, United Kingdom.
57. **Postgate JR, Campbell LL.** 1966. Classification of *Desulfovibrio* species, the non-sporulating sulfate-reducing bacteria. Bacteriol. Rev. **30**:732–738.
58. **Rabus R, Hansen TA, Widdel F.** 2006. Dissimilatory sulfate- and sulfur-reducing prokaryotes, p 659–786. *In* Dworkin M, Falkow S, Rosenberg E, Schleifer KH, Stackbrandt E (ed), The prokaryotes. Springer-Verlag, New York, NY.
59. **Rees CE.** 1973. A steady-state model for sulphur isotope fractionation in bacterial reduction processes. Geochim. Cosmochim. Acta **37**:1141–1162.
60. **Rickard D, Luther GW, III.** 2007. Chemistry of iron sulfides. Chem. Rev. **107**:514–562.
61. **Rudnicki MD, Elderfield H, Spiro B.** 2001. Fractionation of sulfur isotopes during bacterial sulfate reduction in deep ocean sediments at elevated temperatures. Geochim. Cosmochim. Acta **65**:777–789.
62. **Sim MS, Ono S, Donovan K, Templer SP, Bosak T.** 2011. Effect of electron donors on the fractionation of sulfur isotopes by a marine *Desulfovibrio* sp. Geochim. Cosmochim. Acta **75**:4244–4259.
63. **Sim MS, Bosak T, Ono S.** 2011. Large sulfur isotope fractionation does not require disproportionation. Science **333**:74–77.
64. **Stams FJM, Veenhuis M, Weenk GH, Hanssen TA.** 1983. Occurrence of polyglucose as a storage polymer in *Desulfovibrio* species and *Desulfobulbus propionicus.* Arch. Microbiol. **136**:54–59.
65. **Sweeny RE, Kaplan IR.** 1980. Stable isotope composition of dissolved sulfate and hydrogen sulfide in the Black Sea. Mar. Chem. **9**:145–152.
66. **Thode HG, Monster J, Dunford HB.** 1961. Sulphur isotope geochemistry. Geochim. Cosmochim. Acta **25**:158–174.
67. **Wang G, Spivack AJ, D'Hondt S.** 2010. Gibbs energies of reaction and microbial mutualism in anaerobic deep subseafloor sediments of ODP site 1226. Geochim. Cosmochim. Acta **74**:3938–3947.
68. **Widdel F, Kohring GW, Mayer F.** 1983. Studies on dissimilatory sulfate-reducing bacteria that decomposed fatty acids. III. Characterization of the filamentous gliding *Desulfonema limocola* gen. nov. sp. nov. and *Desulfonema magnum* sp. nov. Arch. Microbiol. **134**:286–294.
69. **Wright RT, Coffin RB.** 1984. Measuring microzooplankton grazing on planktonic marine bacteria by its impact on bacterial production. Microb. Ecol. **10**:137–149.